Surface core-level shifts of barium observed in photoemission of vacuum-fractured $BaTiO_3(100)$

L. T. Hudson, R. L. Kurtz,* and S. W. Robey
Surface and Microanalysis Science Division, National Institute of Standards and Technology, Gaithersburg, Maryland 20899

D. Temple and R. L. Stockbauer
Department of Physics and Astronomy, Louisiana State University, Baton Rouge, Louisiana 70803
(Received 27 October 1992; revised manuscript received 8 January 1993)

When clean, vacuum-fractured surfaces of $BaTiO_3$ are analyzed using ultraviolet and x-ray photoelectron spectroscopy (UPS and XPS), more than one set of barium core levels is observed. Sputtering the surface with ions removes lower-binding-energy intensity within the barium line shapes in UPS spectra while little change is noted in XPS. Sputtering of the surface also causes band bending and the creation of band-gap surface states of Ti 3*d* character. From a comparison of UPS and XPS Ba 4*d* line shapes from a vacuum-fractured surface, the lower-binding-energy component is assigned to barium with 12-fold oxygen coordination representative of bulk stoichiometry; the higher-binding-energy intensity originates from undercoordinated barium in the region of the sample surface. Such a negative chemical shift of core levels with increased coordination has been observed in the oxidation of metallic barium as well as in the high-temperature superconductor systems that contain barium. Reasonable values for the energy-dependent attenuation length of electrons in $BaTiO_3$ are derived from the relative intensities of bulk and surface components using a simple model of electron attenuation.

I. INTRODUCTION

It has been shown that cleaning $BaTiO_3$ surfaces by ion sputtering produces a nonstoichiometric surface region[1–4] and that high-temperature annealing of both sputtered[4] and unsputtered[5] samples introduces new features in photoemission spectra. Cleaving oxides *in situ* is the preferred method for obtaining a clean surface which has the stoichiometry of the bulk. Recent studies performed in this laboratory[6] showed that the valence bands from new surface microphases introduced by annealing (as in Ref. 4) do not represent the electronic structure of vacuum-fractured (100) surfaces of barium titanate. Even clean, vacuum-fractured surfaces, however, do not exhibit a single set of barium core levels in photoemission. This is most evident for the Ba 5*p* and 4*d* levels since the magnitude of the core-level shift is comparable with the spin-orbit splitting. With our experimental resolution, these levels typically appeared as a single, unresolved feature. After sputtering the surface with argon ions, this feature narrowed and was resolved into two spin-orbit-split (SOS, also used for "spin orbit splitting") components. These same phenomena have been observed recently in high-temperature superconductors that contain barium. In these systems, photoelectron spectroscopic studies have resulted in conflicting assignments of the two sets of barium features.[7–9] The purpose of the present investigation is to identify which set of barium levels is representative of bulk barium titanate and to determine the physical origin and direction of shift of the other set of core levels.

II. EXPERIMENT

The ultraviolet photoelectron spectroscopy (UPS) measurements were performed using the National Institute of Standards and Technology SURF-II synchrotron light source. These measurements were made with incident photons in the energy range of 30–130 eV delivered by a 3-m toroidal grating monochromator at about 48° to the surface normal. Angle-integrated spectra were obtained with a double-pass cylindrical-mirror analyzer (CMA) operated in the retarding mode with a pass energy of 15 eV. The axis of the CMA was perpendicular to the incident photon direction, and the sample normal was oriented along the mean acceptance angle of the spectrometer ($\approx 42°$) and in the plane defined by the photon beam and the CMA axis. The spectra have been normalized to incident photon flux. The overall resolution was a function of the photon energy and varied from 0.4 eV at $h\nu = 38$ eV to about 1 eV at 130 eV. The energy distribution curves (EDC's) are referenced to the common Fermi level (E_F) of the target-detector system as determined with a sputter-cleaned gold foil. X-ray photoelectron spectra (XPS) were recorded using an Al $K\alpha$ (1486.6 eV) source with an overall experimental resolution of ≈ 1 eV; XPS binding energies were referenced to Au $4f_{7/2} \equiv 84.0$ eV.[10]

The single-crystal $BaTiO_3$ samples used in this study were produced by the top-seeded solution growth technique. When polished they were a transparent yellow. The samples were oriented by x-ray diffraction and cut into rectangular rods with faces normal to the [100] family of axes in the cubic system. Barium titanate is a ferroelectric material with the cubic perovskite crystal structure above its Curie temperature of ≈ 400 K. The crystal structure can be visualized by placing Ba in the center of a cube (4 Å on a side) coordinated by 12 oxygens on the cube edges. Titanium ions on the cube corners then reside in sixfold coordinated cages of oxygen. Below 400 K, $BaTiO_3$ relaxes to tetragonal symme-

try. Reflectivity spectra[11] and band-structure calculations[12] show that this cubic-to-tetragonal transition is accompanied by changes in energy levels of only 10–150 meV. Indeed, our photoemission spectra show no discernible changes in the electronic structure as a function of ferroelectric phase.

Our samples were found to charge excessively under the high photon fluxes of the synchrotron light source. This problem was overcome by chemically reducing the sample by heating *in vacuo*, thus producing an *n*-type semiconductor. From detailed reduction studies of $BaTiO_3$,[13] it is estimated that the reduced samples used in this study (produced by heating to 870–1170 K for about 10 min) contained a carrier concentration of up to $\approx 10^{17}$ electrons/cm^3. The only measurable effect of this reduction technique on the electronic structure is to pin the Fermi level at the bottom of the conduction band; we find the top of the valence band at a binding energy equal to the optical band gap of $BaTiO_3$ which is about 3.3 eV.[14] The binding energies quoted in this paper are with respect to this pinned Fermi level. Some of the lesser-reduced samples exhibited charging of a few volts. This difficulty was routinely overcome by raising the sample temperature to ≥ 360 K. To eliminate any uncertainties due to small residual charging, most of the photoelectron spectra shown here were taken with a sample temperature of ≥ 370 K. If a spectrum was acquired at room temperature, the valence band was aligned to that of a spectrum taken with the same photon energy and from a sample held at elevated temperature. As mentioned above, the high-temperature annealing used for reduction can create new surface microphases which contribute additional features to photoemission spectra. It is, therefore, important to expose a new surface before performing photoemission measurements. Accordingly, the samples of this study were fractured *in vacuo* (typically 3×10^{-10} Torr) after reduction; this procedure generally yielded multifaceted faces with facet normals within a few degrees of the [100] crystallographic axis. The surface thus obtained is initially clean to within the Auger detection limit.

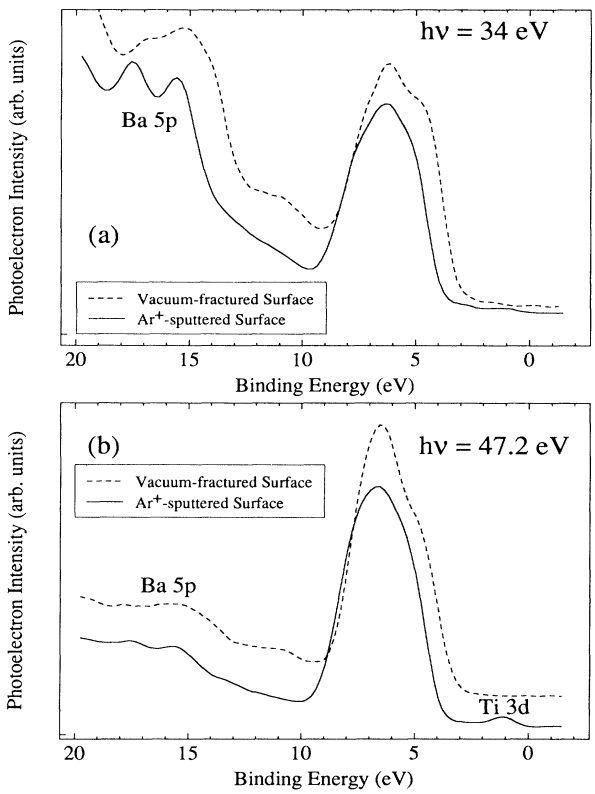

FIG. 1. EDC's from a vacuum-fractured (100) surface of barium titanate before (dashed line) and after (solid line) Ar^+-ion sputtering taken with (a) photon energies below the Ti $3p \rightarrow 3d$ optical-adsorption transition ($h\nu = 34$ eV) and (b) above the Ti $3p \rightarrow 3d$ optical-adsorption transition ($h\nu = 47.2$ eV).

III. RESULTS AND DISCUSSION

Figures 1(a) and 1(b) show EDC's from a vacuum-fractured (100) surface of barium titanate before (dashed line) and after (solid line) Ar^+-ion sputtering and taken with photon energies below (38 eV) and above (47.2 eV) the Ti $3p \rightarrow 3d$ optical-adsorption transition. The valence band extends from about 3 to 9 eV below E_F and is derived primarily from O $2p$ states. The broad feature in the presputtered spectra which lies between 13- and 18-eV binding energy is composed of overlapping, spin-orbit-split doublets due to Ba $5p$ states. The dramatic change in intensity of the Ba $5p$ peaks between Figs. 1(a) and 1(b) is consistent with the rapid fall off of the Ba $5p$ atomic photoionization cross section in this energy range.[15]

As a result of Ar^+-ion sputtering, one observes changes in the electronic structure that were apparent at the minimum fluence used (about 1×10^{15} Ar^+/cm^2 at 500 eV). This evolution had ceased at least by a dose of 9×10^{15} Ar^+/cm^2. Since there are 2.5×10^{15} (ionic surface sites)/cm^2, these ion doses are sufficient to produce a high density of defects at the surface. The most dramatic change accompanying the sputter treatment [Fig. 1(a)] is seen in the Ba $5p$ line shapes; the barium core levels are the main focus of this report and will be discussed below in concert with the other core-level measurements. In addition, inert ion sputtering causes a modification of the valence-band electronic structure, the creation of populated defect states in the band gap, and attendant band bending at the surface of typically ≈ 0.4 eV. Similar effects have also been observed to accompany sputtering of TiO_2 (Refs. 16 and 17) and isoelectronic $SrTiO_3$.[18] Auger-electron spectra showed that the sputtering was accompanied by a relative loss of barium and, to a lesser extent, oxygen in the near-surface region. In the $SrTiO_3$ and TiO_2 systems, the band-gap states have been attributed to the partial population of Ti $3d$ orbitals from adjacent anion vacancies. In $BaTiO_3$ we demonstrate the Ti $3d$ character of these states using the technique of resonant photoemission.

While $BaTiO_3$ is formally a maximal-valent oxide, the covalent bonding is not negligible and resonant photoemission has recently been used to isolate the hybridized

titanium-ligand states of the valence band.[6] Taking advantage of the tunability of the synchrotron light source, one observes resonant emission of photoelectron intensity from the valence-band and band-gap defect states of sputtered $BaTiO_3$ as the incident photon energy is swept through the Ti $3p \rightarrow 3d$ optical-adsorption transition. Excitation from Ti $3p$ to empty Ti $3d$ states can deexcite via direct recombination (or autoionization) and emission from a state with Ti $3d$ character from the valence or defect band (only populated on the sputtered surface). This process interferes with electrons that are photoionized directly from these bands to the continuum.[19] In Fig. 2 the integrated photoelectron intensity above an estimated inelastic background is plotted for the valence and defect bands as a function of photon energy. The background was taken to be proportional to the integrated number of unscattered electrons with higher kinetic energy. The intensity under the circled plot symbols is due in part to Ba $4d$ peaks, produced by third-order light passing through the window of integration. The solid line is drawn as a guide to the eye. This valence-band resonance from a sputtered $BaTiO_3$ surface is similar in shape and position to that found for a vacuum-fractured surface.[6] This resonance is an interatomic decay channel and, for emission from the valence band, is therefore a measure of the Ti $3d$–O $2p$ hybridization in the valence shell of this material. Since the resonance of the band-gap states occurs at the same photon energy as the valence band, we can associate these defect states primarily with charge transfer back to titanium ions and the opening of an intra-atomic Auger decay channel of the same initial excited state.

When identifying the sources of chemically shifted core levels measured by photoemission, one must examine the possible role of gaseous adsorption and/or absorption. If such were the case, the observed removal, by sputtering, of component(s) from Ba core-level line shapes would be explained by the simple removal of this contamination. The adsorption of ambient vacuum gases is indeed detected on these surfaces with the passage of time, but this was found not to affect the line shapes of any of the measured core levels of barium. Figure 3 shows a time-lapse series of EDC's taken from the same vacuum-fractured surface at $h\nu = 40$ eV; the curves have not been scaled or translated with respect to each other. The lower EDC (solid curve labeled $t = 0$) was measured immediately after cleaving the sample. The broad feature from 9 to 12.5 eV is due to Ba $4d$ emissions caused by third-order light as mentioned above. At other photon energies, the region between the Ba $5p$ levels and the valence band is featureless (cf. the sputtered EDC's of Fig. 1). The other spectra were taken (from bottom to top and alternating between dashed and solid lines) at 1, 2.5, and 6 h after the first EDC. A difference spectrum between the 6-h spectrum and the $t = 0$ spectrum (bottom of Fig. 3) shows the growth of two peaks due to adsorption of vacuum gases; the chamber pressure was about 3×10^{-10} Torr. These features could be completely removed by heating the sample to ≥ 520 K. As a result of contamination, the

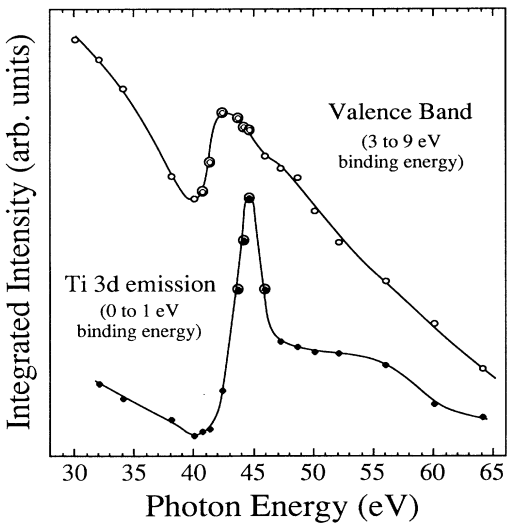

FIG. 2. Integrated photoelectron intensity above inelastic background vs photon energy for the valence band (3–9-eV binding energy) and midgap defect states (0–1-eV binding energy).

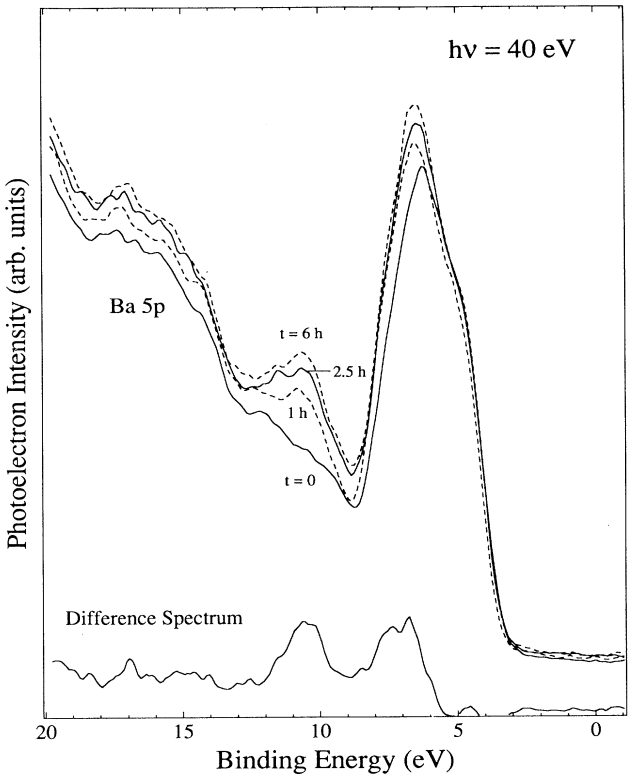

FIG. 3. Photoelectron spectra from a freshly vacuum-fractured $BaTiO_3$ (labeled $t = 0$) and subsequent evolution (elapsed $t = 1$, 2.5, and 6 h) due to the adsorption of ambient vacuum gases. In the lower portion of the figure, the difference spectrum between $t = 6$ h and $t = 0$ demonstrates that ambient contamination does not affect the Ba $5p$ line shape within the time scale of the present experiments.

work function was affected less than 0.1 eV and the only change observed in any core-level line shape was the appearance of a high-binding-energy shoulder on O 1*s*. We conclude that the multiple components exhibited in the core levels of barium are intrinsic to the vacuum-fractured surface of $BaTiO_3$ and are not due to surface or bulk contamination. Photoelectron spectra were taken from samples that exhibited relatively little contamination.

Vacuum-fracturing (100) surfaces of ABO_3 materials with the perovskite crystal structure is expected to produce a stepped surface with variable but approximately equal areas of AO and BO_2 planes. This variation of surface composition from cleave to cleave is consistent with the observed variability of Ba core-level line shapes. We examined over 40 vacuum-fractured surfaces. While there was some variation in the line shape and width of emission from a given barium core level, in all but two cases, there was clearly more than one set of Ba core levels present in the photoemission spectrum. This is easily determined in this system since the core-level shift is of a magnitude such that it causes the ordinarily resolved spin-orbit-split 5*p* and 4*d* levels to overlap, producing a wide, unresolved feature. In the two cases in which well-resolved Ba levels were apparent, an accompanying spectral measurement (either Auger or UPS) showed these surfaces to be relatively poor in Ba. These latter cases may be attributed to statistically improbable cleaves which resulted in a primarily TiO_2-terminated surface. Barium levels also appeared resolved in spectra from unfractured, unreduced, "as-received" samples (measured at elevated temperature to reduce electrostatic charging). In these spectra, the valence region was anomalously broad and featureless; such spectra were never observed on a vacuum-fractured surface. These findings suggest that both samples with bulk-coordinated barium alone and samples with surface barium that are terminated by gross atmospheric contamination could lead to the observation of a single set of barium core levels in photoemission spectra of $BaTiO_3$. Contamination of a vacuum-fractured surface with vacuum gases (which could be cleaned by heating to 520 K) is insufficient to produce a surface that is terminated by the contamination overlayer of an uncleaved surface which had been previously exposed to atmosphere.

Turning now to a discussion of the deeper core levels of barium, Fig. 4 shows the electronic structure of a vacuum-fractured surface of $BaTiO_3$ (100) taken with $h\nu = 130$ eV. The spectrum is dominated by a feature of high cross section due to Ba 4*d* levels; this feature is unresolved on the presputtered surface, as was the case for the Ba 5*p* levels in Fig. 1. The inset of Fig. 4, however, shows the evolution of these 4*d* emissions from a surface which has been irradiated with Ar^+ ions with the incremental dose and energy reported in the figure. The evolution is nearly complete after the initial fluence of about 1×10^{15} Ar^+/cm^2 at 500 eV; by a dose of 9×10^{15} Ar^+/cm^2, the transformation is complete.

A more detailed measurement of the Ba 4*d* line shapes is shown in Fig. 5. For the three line shapes shown, the plotting symbols represent measured intensities after sub-

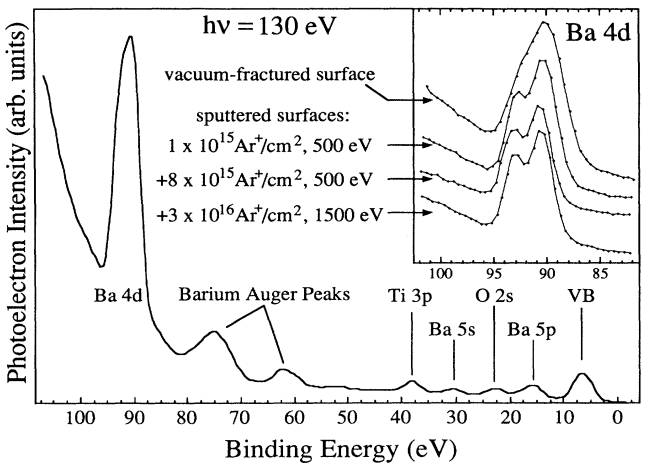

FIG. 4. The electronic structure of a vacuum-fractured surface of $BaTiO_3$ (100) taken with $h\nu = 130$ eV. The inset shows the evolution of the Ba 4*d* emissions from a surface which has been irradiated with Ar^+ ions with the incremental dose and energy reported in the figure.

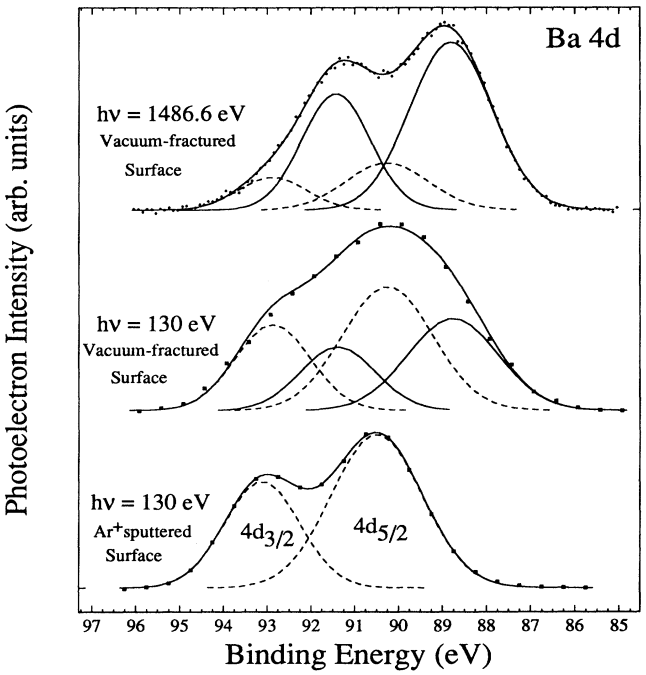

FIG. 5. Barium 4*d* line shapes obtained from a single vacuum-fractured surface of $BaTiO_3$ (100). The unsmoothed data are represented by plotting symbols and the smooth curves represent the sum of the Gaussian functions shown beneath each data set. The top two spectra contrast a bulk-sensitive, XPS measurement with a more surface-sensitive UPS measurement. As discussed in the text, the lower-binding-energy intensity originates from surface or undercoordinated barium. The bottom spectrum was acquired after sputtering the surface with Ar^+ ions. The effect was to remove bulk-coordinated barium from the UPS detection volume. See also the discussion of attenuation lengths in $BaTiO_3$.

traction of a linear background. No smoothing has been performed. The solid lines through the data are the sums of the Gaussian functions shown beneath each data set. The top two curves were taken from the same vacuum-fractured surface using Al $K\alpha$ ($h\nu=1486.6$ eV) and synchrotron light at $h\nu=130$ eV. The lowest curve was also taken at 130 eV but after sputtering this same surface with Ar^+ until there were no more changes in the lineshape. This spectrum was fit to the sum of two Gaussian functions using a least-squares fitting routine. The spin-orbit splitting is 2.6 eV and the ratio of the intensities of the $4d_{5/2}$ and $4d_{3/2}$ components is 1.7. As discussed above, we are motivated to consider both surface- and bulk-coordinated contributions to the Ba core levels on a vacuum-fractured surface. Accordingly, the fit to the vacuum-fractured, *presputtered* 130-eV line shape is highly restricted: these data were fit to the sum of two SOS pairs of Gaussian peaks with the same widths, splitting, and relative amplitudes as that found for the sputtered spectrum; the adjustable parameters were the position and scaling constant for each pair. The XPS data (top curve) are modeled by the deconvolution procedure used for the 130-eV data. This resulted in a 1.5-eV core-level shift between the two pairs of Gaussian functions for both the UPS and XPS spectra of this presputtered, vacuum-fractured surface.

We now compare the top two Ba 4*d* line shapes of Fig. 5 obtained from the same presputtered, vacuum-fractured surface. The data taken at $h\nu=130$ eV, given the restrictions discussed above, could not be fit as the XPS data, i.e., with a relatively large, low-binding-energy SOS pair. In this spectrum, the higher-binding-energy pair dominates. The kinetic energy of the detected 4*d* electrons with respect to the Fermi level is simply the photon energy minus the binding energy (BE). The kinetic energy is about 39 eV for the UPS spectrum and about 1396 eV for the XPS spectrum. Assuming that the relative reversal of high- and low-binding-energy intensity in these two spectra is related to the kinetic energy of the photoemitted electrons and therefore to the relative bulk and surface sensitivity, it is then reasonable and consistent to assign the higher-binding-energy emissions to surface-coordinated barium and the lower to bulk-coordinated barium. We shall refer to the shift between the emissions from the surface and the bulk as the surface core-level shift (SCLS). As discussed earlier, different fractured surfaces gave Ba features with some variation of widths and line shapes. The SCLS and ratio of bulk to surface intensity was then not a constant; however, this ratio was always greatly reduced in the UPS measurements (30–130 eV) relative to that found in the XPS measurements.

Since the line shapes are so well fit to the sum of two sets of SOS pairs and there is only one chemical state associated with bulk-coordinated barium in barium titanate, it would seem that only one undercoordinated chemical state is present. The Ba 4*d* levels remaining in the 130-eV spectrum for the sputtered surface are associated with undercoordinated barium near the sample surface. The result of the ion sputtering must be to eliminate bulk-coordinated barium from the UPS sampling depth by preferentially removing oxygen (a common result of oxide sputtering). This interpretation is enforced by inspection of measured XPS spectra of the Ba 4*d* levels after sputtering (not shown). Rather than a dramatic change in line shape, the only change observed was a few tenths of an electron volt broadening of the line shape. Similar broadening was observed on Ti and O line shapes and is probably caused by changes in oxygen coordination due to oxygen loss.

The disappearance of low-binding-energy barium components upon sputtering has also been observed in the high-T_c superconducting materials that contain barium. One such study concluded that the low-binding-energy components are due to surface coordination. The result of sputtering is then interpreted as removal of all barium from the surface.[8] Other studies have come to the opposite assignment; there now seems to be agreement that the low-binding-energy Ba features are characteristic of the bulk superconductor.[7,9] Indeed, a recent study of $YBa_2Cu_3O_{7-\delta}$ which was chemically etched leaving the surface terminated in Cu-O planes found the higher-binding-energy species absent in the Ba 4*d* photoemission spectrum.[20]

As a consistency check, the Ba 5*p* levels (sputtered and unsputtered) from Fig. 1 with a straight-line background subtracted are fit in Fig. 6 using the same procedure as with the Ba 4*d* levels. The $h\nu=34$ eV spectra are used because of the higher photoionization cross section; even so the counting statistics are worse than the Ba 4*d* data and the fit is poorer. The ratio of the $5p_{3/2}$ to $5p_{1/2}$ peak areas is found to be about 1.6. For this spectrum, the SOS is 1.9 eV and the SCLS is 1.0 eV. The ratio of surface-to-bulk intensity is here about one, perhaps reflecting the increased bulk sensitivity common at very low kinetic energies ($h\nu-$BE). This observation suggests using the ratio of the derived surface and bulk intensities to estimate the electron attenuation length (AL) for single-crystal $BaTiO_3$ at several kinetic energies.

As a first approximation, a discrete-layer model of electron attenuation will be used. This model assumes uniform illumination through the depth of the sample and similar atomic densities in the surface and bulk regions. The detected photoelectron intensity originating from a surface region of thickness t will then be proportional to the integral from 0 to t over the thickness variable z of $e^{-z/\lambda\cos\theta}$ where λ is the AL of electrons of a given kinetic energy and θ is the angle between the surface normal and mean acceptance angle of the electron energy analyzer. The photoelectron intensity from the bulk ($z>t$) is proportional to a similar integral to infinite depth with a further attenuation factor due to ultimate passage through the surface region: $e^{-t/\lambda\cos\theta}$. The ratio of intensity from the surface, I_S, and the bulk, I_B, is then given by

$$\frac{I_S}{I_B}=\frac{\int_0^t e^{-z/\lambda\cos\theta}dz}{\left[\int_0^\infty e^{-z/\lambda\cos\theta}dz\right]e^{-t/\lambda\cos\theta}}$$
$$=e^{+t/\lambda\cos\theta}-1\ .$$

The thickness of the surface region is taken to be that of the unit cell of $BaTiO_3$, which is 4 Å. This estimate in-

cludes barium in the top atomic plane for regions of the surface that are terminated with BaO and, in regions of the surface which are terminated with TiO_2, barium in the second atomic plane which is not fully coordinated because of vacancies in the surface plane. In our experimental geometry, $\cos\theta$ is ≈ 1. One can then solve for λ by integrating the intensity of the deconvolved line shapes in Figs. 5 and 6 assuming one set to originate in a surface region of undercoordinated barium and the other from a region of bulk-coordinated barium. $\lambda=\lambda(\mathrm{KE})$ where KE is the kinetic energy of the ejected electron with respect to the Fermi level and is given by $\mathrm{KE}=h\nu-\mathrm{BE}$.

If the high-binding-energy set of barium core levels is due to surface or undercoordinated barium, then from the deconvolved Ba $4d$ line shapes (presputtered) of Fig. 5, $I_S/I_B=0.3$ for the XPS spectrum and is 1.3 for the 130-eV spectrum; we then find $\lambda(1396\ \mathrm{eV})=15$ Å and $\lambda(39\ \mathrm{eV})=5$ Å, respectively. If, instead, the high-binding-energy set of levels was assumed to arise from bulk-coordinated barium, then we find $\lambda(1396\ \mathrm{eV})=3$ Å and $\lambda(39\ \mathrm{eV})=7$ Å. The former assignment is much more characteristic of the AL behavior of inorganic materials[21] and, as mentioned previously, more in agreement with the expectation that the XPS measurements have greater bulk sensitivity. The deconvolution of the presputtered Ba $5p$ line shape in Fig. 6 indicated that the high- and low-binding-energy components had about equal intensities. This result leads to $\lambda(18\ \mathrm{eV})=6$ Å which is consistent with the expected increasing bulk sensitivity at very low kinetic energies. The Ba core levels, SOS, and SCLS's are summarized in Table I. The figures quoted for the core-level binding energies are the mean values from the results of fits for different vacuum-fractured surfaces. The peak positions thus obtained varied from the mean values by ≤ 0.3 eV.

The Ba $3d$ levels exhibited a high-binding-energy shoulder on each SOS component. The SOS components could not be uniquely deconvolved into "surface" and "bulk" peaks. The discrete-layer model predicts that, at this final-state kinetic energy (around 707 eV for Ba $3d_{5/2}$) the ratio of bulk-to-surface intensity should be about two to one. Fitting with this restriction resulted in a SCLS of 1.4 eV for each SOS component. This procedure is not considered as giving bulk Ba $3d$ binding energies (listed in Table I) of particularly high accuracy. It is encouraging, however, that the difference in the Ba $3d_{5/2}$ and Ba $4d_{5/2}$ bulk binding energies, 690.3 eV, compares favorably with the value found for a large group of ionic barium compounds, 690.4 eV.[22]

In general, it is difficult *a priori* to predict whether the core levels of a metal will move away from or toward the

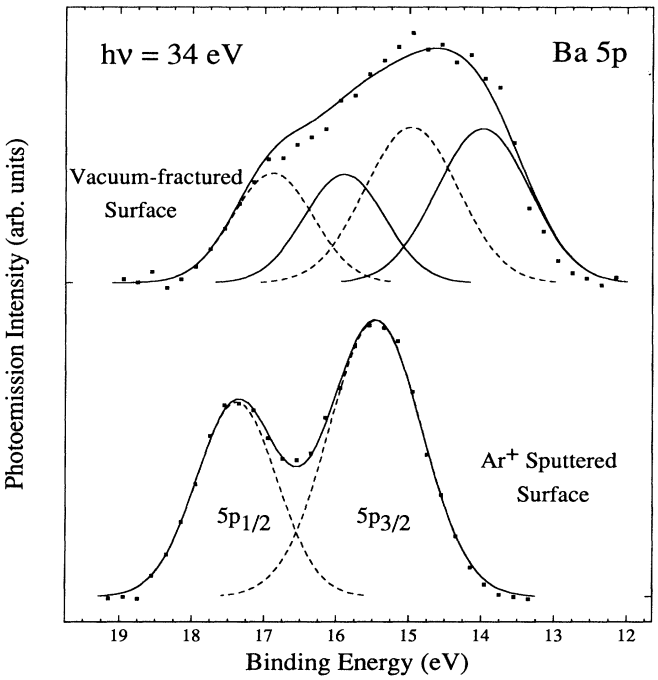

FIG. 6. Barium $5p$ line shapes taken from the EDC's of Fig. 1 after subtracting a linear background. The unsmoothed data are represented by plotting symbols and the smooth curves represent the sum of the Gaussian functions shown beneath each data set.

TABLE I. Comparison of barium core-level spectroscopy from $BaTiO_3$, Ba, and oxidized Ba.

Barium core level	Vacuum-fractured $BaTiO_3$ Core-level BE (eV)[b] Bulk	Surface	SCLS (eV)	SOS[c] (eV)	Bulk Ba[a] BE (eV)	SOS (eV)	Ba+8.4 L O_2[a] BE (eV)	SOS (eV)
$5p_{3/2}$	14.3	15.4	1.1	1.9	14.6	2.28	14.2	1.9
$4d_{5/2}$	89.2	90.5	1.3	2.6	89.8	2.68	89.2	2.68[d]
$3d_{5/2}$	779.5	780.9	1.4	15.3				15.4[e]

[a]From Ref. 23.

[b]The binding energy of the core levels of $BaTiO_3$ are referenced from the Fermi level which, due to reduction of the sample, is pinned at the top of the band gap (about 3.3 eV). The values quoted are averaged over the results of fits from different vacuum-fractured surfaces. The peak positions thus obtained varied from this mean value by ≤ 0.3 eV.

[c]Spin-orbit splitting is determined by least-squares fitting of the line shapes from sputtered samples to the sum of two Gaussian functions.

[d]Value at 2.4 L of O_2 exposure.

[e]For BaO from Ref. 24.

Fermi level as it is oxidized. As charge is transferred to the oxygen ligand, the electrostatic potential at the cationic site increases (an initial-state effect) and the intraatomic and interatomic relaxation screening of the core hole (final-state effects) are reduced as the host transforms from metallic to insulating. Each of these effects would cause a shift of a core-level photoemission line away from the Fermi level, a so-called positive chemical shift. Increasing the oxygen coordination in a metallic host can cause negative chemical shifts of the metal core levels by increasing the negative Madelung potential at the cationic site (an initial-state, electrostatic effect) and by increased polarization screening of the final state by the increased number of oxygen ligands (a final-state effect). The core levels of barium metal exhibit a negative chemical shift and a reduction of SOS as it is oxidized and bulk BaO is formed (see Table I).[23] Again, this trend is consistent with our assignment of the lower-binding-energy core levels with bulk oxygen coordination. This effect has been attributed to polarization screening of the final state by O $2p$ states of the anion.[23] While this screening is probably a contributing factor to the negative chemical shift of barium, Vasquez[22] has studied a number of ionic compounds containing barium and found that there is no systematic correlation between the magnitude of the chemical shift and the degree of polarizability of the anion. The negative shift is attributed primarily to the large negative Madelung energies at the cationic sites which is common in ionic materials.

IV. SUMMARY

We have presented a photoelectron spectroscopic study of the barium core levels of vacuum-fractured, single-crystal $BaTiO_3$. The observation of more than one set of core levels is attributed to a surface-core-level shift to higher binding energies due to barium near the surface which is undercoordinated by oxygen. This assignment parallels conclusions reached in studies of barium-containing high-temperature superconducting materials which, like barium titanate, possess the cubic perovskite crystal structure. The ratio of surface-to-bulk components was used with a simple discrete-layer model of electron attenuation to predict reasonable values for the electron attenuation length for electrons in $BaTiO_3$ for several kinetic energies. Our results are consistent with published trends of AL variations with energy for inorganic materials.[21]

ACKNOWLEDGMENT

The authors gratefully acknowledge the assistance and technical support of the staff of the NIST SURF-II synchrotron.

*Present address: Department of Physics and Astronomy, Louisiana State University, Baton Rouge, LA 70803.

[1]F. L. Battye, H. Höchst, and A. Goldmann, Solid State Commun. **19**, 269 (1976).

[2]P. Pertosa and F. M. Michel-Calendini, Phys. Rev. B **17**, 2011 (1978).

[3]R. Courths, Phys. Status Solidi B **100**, 135 (1980).

[4]B. Cord and R. Courths, Surf. Sci. **152/153**, 1141 (1985).

[5]B. B. Leikina, M. A. Kvantov, and Yu. P. Kostikov, Izv. Akad. Nauk SSSR, Neorg. Mater. **16**, 135 (1991).

[6]L. T. Hudson, R. L. Kurtz, S. W. Robey, D. Temple, and R. L. Stockbauer, Phys. Rev. B **47**, 1174 (1993).

[7]N. G. Stoffel, P. A. Morris, W. A. Bonner, D. LaGraffe, M. Tang, Y. Chang, G. Margaritondo, and M. Onellion, Phys. Rev. B **38**, 213 (1988).

[8]R. Liu, C. G. Olson, A.-B. Yang, C. Gu, D. W. Lynch, A. J. Arko, R. S. List, R. J. Bartlett, B. W. Veal, J. Z. Liu, A. P. Paulikas, and K. Vandervoort, Phys. Rev. B **40**, 2650 (1989).

[9]D. E. Fowler, C. R. Brundle, J. Lerczak, and F. Holtzberg, J. Electron Spectrosc. Relat. Phenom. **52**, 323 (1990).

[10]M. P. Seah, Surf. Interface Anal. **14**, 488 (1989).

[11]M. Cardona, Phys. Rev. **140**, A651 (1965); D. Bäuerle, W. Braun, V. Saile, G. Sprüssel, and E. E. Koch, Z. Phys. B **29**, 179 (1978).

[12]F. M. Michel-Calendini and G. Mesnard, Phys. Status Solidi **44**, K117 (1971); J. Phys. C **6**, 1709 (1973).

[13]J. Dubuisson and P. Basseville, in *The Role of Grain Boundaries and Surfaces in Ceramics,* Materials Science Research Vol. 3, edited by W. W. Kriegel and H. Palmour III (Plenum, New York, 1966), p. 77.

[14]S. H. Wemple, Phys. Rev. B **7**, 2679 (1970).

[15]J. J. Yeh and I. Lindau, At. Data Nucl. Data Tables **32**, 1 (1985) (see, especially, pp. 10 and 76).

[16]V. E. Henrich, G. Dresselhaus, and H. J. Zeiger, Phys. Rev. Lett. **36**, 1335 (1976).

[17]Z. Zhang, S. Jeng, and V. Henrich, Phys. Rev. B **43**, 12 004 (1991).

[18]V. E. Henrich, G. Dresselhaus, and H. J. Zeiger, Phys. Rev. B **17**, 4908 (1978).

[19]L. C. Davis, J. Appl. Phys. **59**, R25 (1986); E. Bertel, R. Stockbauer, and T. E. Madey, Phys. Rev. B **27**, 1939 (1983); Surf. Sci. **141**, 355 (1984).

[20]R. P. Vasquez, M. C. Foote, L. Bajuk, and B. D. Hunt, J. Electron Spectrosc. Relat. Phenom. **57**, 317 (1991).

[21]M. P. Seah and W. A. Dench, Surf. Interface Anal. **1**, 2 (1979).

[22]R. P. Vasquez, J. Electron Spectrosc. Relat. Phenom. **56**, 217 (1991).

[23]K. Jacobi, C. Astaldi, B. Frick, and P. Geng, Phys. Rev. B **36**, 3079 (1987).

[24]C. D. Wagner, W. M. Riggs, L. E. Davis, and J. F. Moulder, in *Handbook of X-ray Photoelectron Spectroscopy,* edited by G. E. Muilenberg (Perkin-Elmer, Eden Prairie, 1979), p. 130.